

Complexes of 2-hydroxy-5-methyl-1,4-benzoquinone as models for the 'TPQ-on' form of copper amine oxidases

Caroline L. Foster, Xiaoming Liu, Colin A. Kilner, Mark Thornton-Pett and Malcolm A. Halcrow*

School of Chemistry, University of Leeds, Woodhouse Lane, Leeds, UK LS2 9JT.

E-mail: M.A.Halcrow@chem.leeds.ac.uk

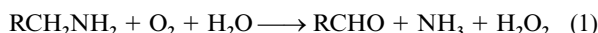
Received 16th August 2000, Accepted 24th October 2000

First published as an Advance Article on the web 1st December 2000

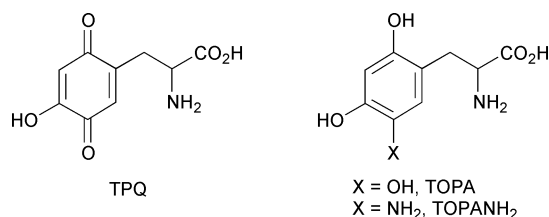
Reaction of hydrated CuCl_2 with equimolar amounts of $\text{Na}[\text{L}^1] \cdot \text{H}_2\text{O}$ ($\text{HL}^1 = 2\text{-hydroxy-5-methyl-1,4-benzoquinone}$) and $\text{K}[\text{Tp}^{\text{Ph}_2}]$ ($[\text{Tp}^{\text{Ph}_2}]^- = \text{tris-[3,5-diphenylpyrazol-1-yl]hydridoborate}$) in CH_2Cl_2 at room temperature afforded $[\text{Cu}(\text{L}^1)(\text{Tp}^{\text{Ph}_2})] \mathbf{1}$ in moderate yields. A similar complexation employing hydrated $\text{Zn}(\text{BF}_4)_2$, $\text{Na}[\text{L}^1] \cdot \text{H}_2\text{O}$ and $\text{K}[\text{Tp}^{\text{Ph}_2}]$ in refluxing CH_2Cl_2 affords $[\text{Zn}(\text{L}^1)(\text{Tp}^{\text{Ph}_2})] \mathbf{2}$. The single crystal structure of $\mathbf{1} \cdot 0.8\text{CH}_2\text{Cl}_2$ reveals a near-regular square pyramidal copper(II) centre, with a chelating $[\text{L}^1]^-$ ligand. In contrast, the structure of $\mathbf{2}$ shows a distorted trigonal bipyramidal geometry, with a long interaction to the chelating carbonyl O donor. IR, UV/vis, NMR and/or EPR data demonstrate that $\mathbf{1}$ and $\mathbf{2}$ adopt the same molecular structures in CH_2Cl_2 solution as in the solid state. The cyclic voltammogram of $\mathbf{2}$ in CH_2Cl_2 -0.5 M NBu_4BF_4 at 293 K exhibits chemically reversible 1-electron $[\text{L}^1]^- - [\text{L}^2]^{2-}$ and $[\text{L}^2]^{2-} - [\text{L}^3]^{3-}$ ($\text{H}_2\text{L}^2 = 2\text{-hydroxy-5-methyl-1,4-semiquinone}$; $\text{H}_3\text{L}^3 = 2,4,5\text{-trihydroxy-toluene}$) couples. The CV of $\mathbf{1}$ under these conditions is more complex, showing an irreversible $\text{Cu}^{\text{II}} - \text{Cu}^{\text{I}}$ couple, with daughter waves that suggest that reduction of the Cu in $\mathbf{1}$ results in decomplexation of $[\text{L}^1]^-$. These results imply that a previously proposed stepwise mechanism for the oxidative half-reaction of copper-containing amine oxidase may only take place if the enzyme's hydroquinone cofactor is coordinated to the active site copper ion.

Introduction

Copper-containing amine oxidases (CAOs), which catalyse the aerobic oxidation of primary amines (eqn. 1), have been



isolated from bacterial, yeast, plant and mammalian sources, including humans.¹ The active site of CAO contains a type 2 $[\text{Cu}(\text{his})_3(\text{OH}_2)_n]^{+/2+}$ ($n = 0$ or 2) centre,²⁻⁶ and the protein-bound cofactor 2-(1-amino-1-carboxyethyl)-5-hydroxy-1,4-benzoquinone (TPQ),⁷ which is derived from a post-translational self-processing modification of a tyrosine side-chain.⁸ Crystal structures of different CAOs contain the TPQ cofactor either lying 3–5 Å from the Cu ('TPQ-off', Fig. 1a), or directly coordinated to the Cu ('TPQ-on', Fig. 1b). The TPQ-off form represents the resting state of a catalytically active CAO molecule, and it is presently uncertain whether coordination of the TPQ residue to the Cu takes place during catalytic turnover.



Catalysis by CAO is believed to follow a ping-pong mechanism, involving distinct reductive and oxidative half-reactions (eqns. 2 and 3). The TPQ residue is the site of amine oxidation, which takes place by an aminotransferase mechanism and

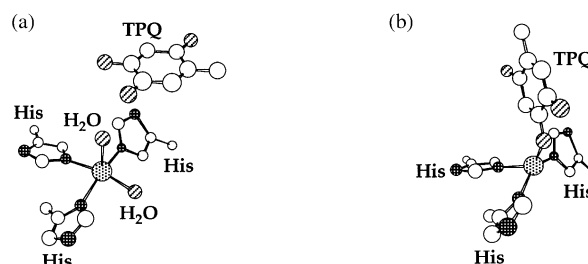
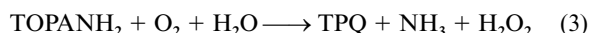
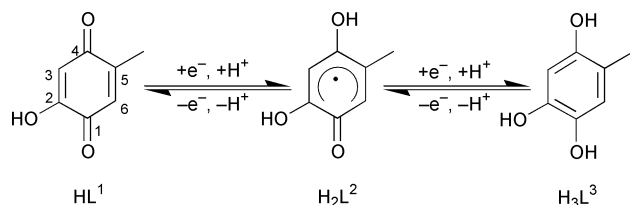


Fig. 1 Views of the TPQ-off (a) and TPQ-on (b) forms of the active site of copper amine oxidase.

affords the reduced cofactor 5-amino-2,4-dihydroxyphenylalanine (TOPANH₂, eqn. 2).⁸⁻¹¹ The copper site of CAO appears to be involved in reoxidation of the substrate-reduced cofactor (eqn. 3). Consistent with this, it is known that one-electron transfer between the copper ion and reduced cofactor can take place at catalytically competent rates.¹² It is not known whether coordination of the cofactor to the copper ion is required for this electron transfer to take place, however. In addition, the relevance of this electron-transfer reaction to cofactor reoxidation during catalysis has recently been disputed,¹³ so that the function of the CAO copper center is still open to question.

Since little model chemistry for the CAO copper site has been published to date,¹⁴⁻¹⁶ we have embarked on a program to prepare new copper(II)/quinone or hydroquinone complexes in order to address these questions.¹⁷ This is a complement to our continuing work on model chemistry for the copper/radical enzyme galactose oxidase.¹⁸ We describe here complexes of Cu^{II} and Zn^{II} containing 2-hydroxy-5-methyl-1,4-benzoquinone (HL^1 , Scheme 1), intended to model structurally and electrochemically the Cu/TPQ interactions in CAO. Thus far no complex of $[\text{L}^1]^-$ has been described. However, the electrochemistry



Scheme 1 2-Hydroxy-5-methyl-1,4-benzoquinone (HL^1) and derivatives referred to in this work. The IUPAC atom numbering scheme for HL^1 is shown (note that this is not the same as the atom numbering convention used for TPQ). Note that the abbreviations HL^1 , H_2L^2 and H_3L^3 refer to the quinone, semiquinone and hydroquinone redox states of the 2-hydroxy-5-methyl-1,4-benzoquinone ligand, respectively.

of one complex of its fully reduced congener 1,2,4-trihydroxy-5-methylbenzene (H_3L^3 , Scheme 1) has been reported, $\text{Na}[\text{Ru}(\text{L}^3)(\text{bipy})_2] \cdot 2\text{EtOH}$, along with the EPR spectrum of the oxidation product $[\text{Ru}(\text{L}^3)(\text{bipy})_2]$.¹⁶ The Trofimenko system of nomenclature for tris-pyrazolylborate ligands¹⁹ is employed throughout the following discussion.

Results and discussion

Complex synthesis and spectroscopic characterisation

The quinone HL^1 was prepared according to the literature method.²⁰ Dry HL^1 is very sensitive to heat and light, making it difficult to handle. However, deprotonation of freshly precipitated HL^1 with NaOH in 1:1 MeCN-MeOH affords a deep red, sparingly soluble sodium salt analysing as $\text{Na}[\text{L}^1] \cdot \text{H}_2\text{O}$, which can be dried and stored at room temperature without special precautions. Both the ^1H and ^{13}C NMR spectra of this salt in $(\text{CD}_3)_2\text{SO}$ show the expected number of resonances for the $[\text{L}^1]^-$ anion, while IR spectroscopy shows four strong peaks in the double bond region, at 1557, 1562, 1638 and 1672 cm^{-1} . By comparison with the vibrational spectra of other hydroxybenzoquinones,²¹ we can assign the 1672 cm^{-1} peak to the $\text{C}=\text{O}$ vibration of $[\text{L}^1]^-$ and either the 1557 or 1562 cm^{-1} peak to the $\text{C}=\text{O}$ vibration (Scheme 1). The other two peaks in this region presumably correspond to $\text{C}=\text{C}$ vibrational modes. The UV/vis spectrum of $\text{Na}[\text{L}^1] \cdot \text{H}_2\text{O}$ in MeCN exhibits $\pi \rightarrow \pi^*$ transitions at $\lambda_{\text{max}} = 216$ ($\epsilon_{\text{max}} = 2400 \text{ M}^{-1} \text{ cm}^{-1}$) and 263 nm (sh), and a $n \rightarrow \pi^*$ transition at $\lambda_{\text{max}} = 515$ nm ($140 \text{ M}^{-1} \text{ cm}^{-1}$).²² The latter peak is red-shifted by 15–25 nm compared to previously reported UV/vis spectra for $[\text{L}^1]^-$ or related 5-alkyl-2-hydroxybenzoquinone anions.^{11,23} This may reflect co-ordination of $[\text{L}^1]^-$ to the Na^+ cation, and/or the absence of hydrogen-bonding interactions, in this solvent (the literature spectra were run in aqueous solution).

We have previously found the $[\text{Cu}(\text{Tp}^{\text{Ph}})]^+$ ($[\text{Tp}^{\text{Ph}}]^-$ = hydridotris(3-phenylpyrazolyl)borate) fragment to be excellent at binding bidentate redox active ligands, and for stabilising their 1-electron redox products.^{17,24} Therefore, we pursued the synthesis of complexes of type $[\text{Cu}(\text{L}^1)(\text{Tp}^{\text{R}})]$ ($[\text{Tp}^{\text{R}}]^-$ = tris-(3-arylpyrazolyl)hydridoborate), in order to investigate the redox chemistry of coordinated $[\text{L}^1]^-$. The synthesis of $[\text{Cu}(\text{L}^1)(\text{Tp}^{\text{Ph}2})]$ **1** was achieved in moderate yield from the reaction of equimolar amounts of $\text{CuCl}_2 \cdot 2\text{H}_2\text{O}$, $\text{Na}[\text{L}^1] \cdot \text{H}_2\text{O}$ and $\text{K}[\text{Tp}^{\text{Ph}2}]$ ($[\text{Tp}^{\text{Ph}2}]^-$ = tris-(3,5-diphenylpyrazolyl)hydridoborate) in CH_2Cl_2 at room temperature, followed by filtration and concentration of the reaction mixture and addition of a large excess of hexanes. The compound $[\text{Zn}(\text{L}^1)(\text{Tp}^{\text{Ph}2})]$ **2** was also prepared by a similar reaction using hydrated $\text{Zn}(\text{BF}_4)_2$, in refluxing CH_2Cl_2 , as an aid towards the interpretation of the electrochemical behaviour shown by **1** (see below).

The Nujol mull IR spectrum of complex **1** exhibits four medium intensity vibrations in the double bond region attributable to coordinated $[\text{L}^1]^-$, at 1645, 1614, 1599 and 1582 cm^{-1} . Since some of these bands lie at substantially lower wavenumber compared to those of $\text{Na}[\text{L}^1] \cdot \text{H}_2\text{O}$, their detailed assignment as $\text{C}=\text{O}$ or $\text{C}=\text{C}$ vibrational modes is not feasible.

Importantly, however, the double bond region of the IR spectrum of **1** in CH_2Cl_2 solution is superimposable upon its Nujol mull spectrum, the peak energies in solution and the solid state being equal to within $\pm 2 \text{ cm}^{-1}$. The similarity of these spectra very strongly suggests that the molecular structures of **1** in solution and in the solid state are the same.

The UV/vis spectrum of complex **1** in CH_2Cl_2 has a similar form to that of $\text{Na}[\text{L}^1] \cdot \text{H}_2\text{O}$, exhibiting peaks at $\lambda_{\text{max}} = 315$ (sh) and 526 nm ($\epsilon_{\text{max}} = 1700 \text{ M}^{-1} \text{ cm}^{-1}$) that can be attributed to the $[\text{L}^1]^-$ ligand. Although a d-d maximum for a $[\text{Cu}^{\text{II}}(\text{Tp}^{\text{R}})\text{L}_2]^{x+}$ centre would be expected close to 670 ± 30 nm,^{18,24} this is presumably masked here by the high-wavelength $[\text{L}^1]^- n \rightarrow \pi^*$ band. That this high-wavelength band is approximately ten times more intense for **1** than for $\text{Na}[\text{L}^1] \cdot \text{H}_2\text{O}$ suggests that this absorption envelope may contain a charge transfer component overlaying the $[\text{L}^1]^- n \rightarrow \pi^*$ absorption. The almost equal intensities of this peak for **1** and the zinc(II) complex **2** (see below) rules out the presence of a LMCT component to this band; the presence of MLCT transition(s) within this envelope cannot be ruled out, however.

The X-band EPR spectrum of complex **1** in CH_2Cl_2 shows the expected 4-line signal from coupling to $^{63,65}\text{Cu}$ ($I = \frac{3}{2}$) at room temperature, with $\langle g \rangle = 2.17$ and $\langle A \{^{63,65}\text{Cu}\} \rangle = 56 \text{ G}$. In CH_2Cl_2 at 140 K, or as a neat powder at 140 K, **1** exhibits the pseudo-axial spectra typical of a tetragonal $\{d_{x^2-y^2}\}^1$ or $\{d_{xy}\}^1$ copper(II) ion [in CH_2Cl_2 $g_{\parallel} = 2.29$, $g_{\perp} = 2.07$, $A_{\parallel} \{^{63,65}\text{Cu}\} = 136 \text{ G}$; as a powder $g_{\parallel} = 2.31$, $g_{\perp} = 2.08$, $A_{\parallel} \{^{63,65}\text{Cu}\} = 135 \text{ G}$]. The similarity of the powder and frozen solution spectra again implies that the molecular structures of **1** are the same in the solid state and in solution. However, while the g values **1** are similar to those of other $[\text{CuL}(\text{Tp}^{\text{Ph}})]$ (L = bidentate ligand) complexes we have studied; the A_{\parallel} coupling for **1** is unusually small.^{17,24} Given that the crystal structure of **1** exhibits no unusual features compared to our previous compounds (see below), the reason for this difference is unclear.

The Nujol mull IR spectrum of complex **2** differs somewhat from **1**, the $\text{C}=\text{O}$ and $\text{C}=\text{C}$ peaks appearing at 1658, 1628, 1587 and 1546 cm^{-1} . The visible spectrum in CH_2Cl_2 is also different from that of **1**, with $\lambda_{\text{max}} = 469$ nm ($\epsilon_{\text{max}} = 1460 \text{ M}^{-1} \text{ cm}^{-1}$). Both these observations imply that the coordination mode of $[\text{L}^1]^-$ is different for **2** compared to that of **1**. As for **1**, the double bond region of the IR spectrum of **2** in CH_2Cl_2 shows only small differences compared to the solid state spectrum, which suggests that the solid state and solution structures of **2** are similar. The ^1H and ^{13}C NMR spectra of **2** in CD_2Cl_2 are consistent with the proposed 1:1 $[\text{Tp}^{\text{Ph}2}]^- : [\text{L}^1]^-$ stoichiometry and show 3-fold symmetry of the $[\text{Tp}^{\text{Ph}2}]^-$ ligand. Although this is inconsistent with the crystal structure of **2** (see below), it is typical behaviour for zinc(II) trispyrazolylborate complexes and reflects fluxionality of **2** in solution.²⁵ Interestingly, 10 peaks assignable to $[\text{Tp}^{\text{Ph}2}]^-$ phenyl C environments were present in the ^{13}C spectrum. This is the number expected if rotation of either the 3- or 5-phenyl substituent of each pyrazole ring is hindered, while the other phenyl group has free rotation. The ^{13}C spectra of some other complexes of $[\text{Tp}^{\text{Ph}2}]^-$ also exhibit this feature.²⁶

Single crystal structures

Single crystals of complexes **1** and **2** of X-ray quality were grown from CH_2Cl_2 -hexanes at -30°C . Both structures contain one complex molecule per asymmetric unit, lying on a general position. In **1** the Cu^{II} adopts a distorted square-pyramidal geometry as seen for other $[\text{CuL}_2(\text{Tp}^{\text{R}})]^{x+}$ complexes (L = monodentate ligand, or L_2 = bidentate ligand; $[\text{Tp}^{\text{R}}]^- = [\text{Tp}^{\text{Ph}}]^-$ or another tris(3-substituted pyrazolyl)borate; $x = 0$ or 1),^{17,24,27} with a lengthened apical $\text{Cu}(1)-\text{N}(2)$ bond of 2.232(2) Å (Fig. 2, Table 1). The $[\text{L}^1]^-$ ligand is bound asymmetrically, with the $\text{Cu}-\text{O}(54)$ distance of 1.931(2) Å being shorter than $\text{Cu}(1)-\text{O}(55)$ at 2.051(2) Å. This is a consequence of the increased

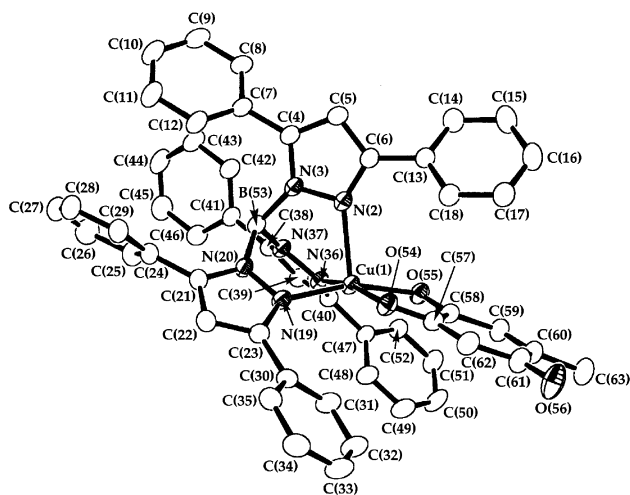


Fig. 2 Structure of the $[\text{Cu}(\text{L}^1)(\text{Tp}^{\text{Ph}_2})]$ complex molecule in the crystal of $1 \cdot 0.8\text{CH}_2\text{Cl}_2$, showing the atom numbering scheme adopted (see also Fig. 4). For clarity, all H atoms have been omitted. Thermal ellipsoids are drawn at the 35% probability level.

Table 1 Selected bond lengths (Å) and angles (°) for the single crystal structures

	$[\text{Cu}(\text{L}^1)(\text{Tp}^{\text{Ph}_2})] \cdot 0.8\text{CH}_2\text{Cl}_2$ (M = Cu)	$[\text{Zn}(\text{L}^1)(\text{Tp}^{\text{Ph}_2})] \cdot 2$ (M = Zn)
M(1)–N(2)	2.232(2)	2.129(3)
M(1)–N(19)	1.997(2)	2.046(3)
M(1)–N(36)	1.982(2)	2.021(3)
M(1)–O(54)	1.931(2)	1.912(3)
M(1)–O(55)	2.051(2)	2.388(3)
N(2)–M(1)–N(19)	94.72(9)	90.16(11)
N(2)–M(1)–N(36)	88.99(9)	89.60(10)
N(2)–M(1)–O(54)	103.41(9)	105.07(11)
N(2)–M(1)–O(55)	103.41(9)	176.59(11)
N(19)–M(1)–N(36)	88.37(10)	97.91(11)
N(19)–M(1)–O(54)	93.80(9)	129.50(13)
N(19)–M(1)–O(55)	161.86(9)	92.39(10)
N(36)–M(1)–O(54)	167.17(9)	129.28(13)
N(36)–M(1)–O(55)	92.62(9)	87.81(10)
O(54)–M(1)–O(55)	81.42(8)	74.98(10)

basicity of the enoxide atom O(54) compared to the carbonyl donor O(55). The asymmetric $[\text{L}^1]^-$ coordination mode is also reflected in the *trans* influence exerted by these O donors on the basal Cu–N distances, in that the bond *trans* to O(54) [Cu(1)–N(36) 1.982(2) Å] is significantly shorter than that *trans* to O(55) [Cu(1)–N(19) 1.997(2) Å]. Given that the enoxide donor O(54) should have π -donor characteristics, this trend suggests that the $[\text{Tp}^{\text{Ph}_2}]^-$ pyrazole donors possess some π -acceptor capability. The Addison and Reedijk ‘ τ ’ parameter for **1** is 0.09, consistent with its near-regular square pyramidal geometry.²⁸

In contrast to complex **1**, the $[\text{L}^1]^-$ ligand in **2** is bound very asymmetrically, with a short bond to the enoxide O donor [Zn(1)–O(54) 1.912(3) Å] and a longer interaction to the chelating carbonyl donor [Zn(1)–O(55) 2.388(3) Å] (Fig. 3, Table 1). The coordination geometry at Zn(1) can therefore be considered as trigonal pyramidal, with N(2) apical, or as trigonal bipyramidal with N(2) and O(55) as the axial donors. Given the near linearity of the N(2)–Zn(1)–O(55) angle [176.59(11)°], the latter description is probably more appropriate. Consistent with this, τ for **2** is 0.78, compared to the limiting value of 1.0 for a trigonal bipyramidal geometry²⁸ ($[\text{ZnL}_2(\text{Tp}^{\text{R}})]^{2+}$ complexes with $\tau = 0.21$ –0.78 have been reported previously^{25,29}).

Consideration of the metric parameters within the bound $[\text{L}^1]^-$ ligands shows that in both structures $[\text{L}^1]^-$ has the elec-

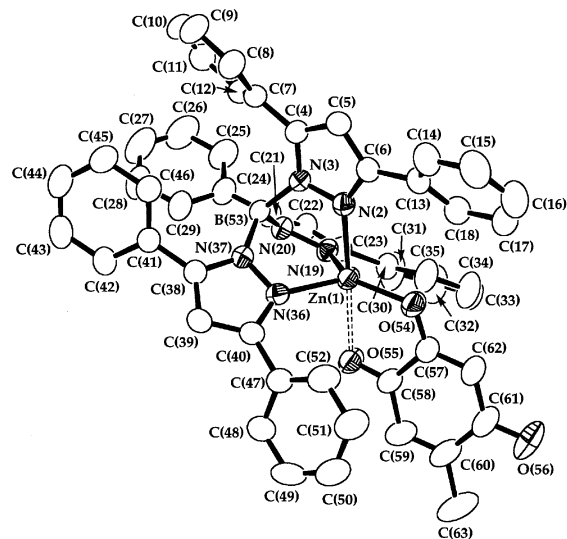


Fig. 3 Structure of the $[\text{Zn}(\text{L}^1)(\text{Tp}^{\text{Ph}_2})]$ complex molecule in the crystal of **2**, showing the atom numbering scheme adopted (see also Fig. 4). Details as for Fig. 2.

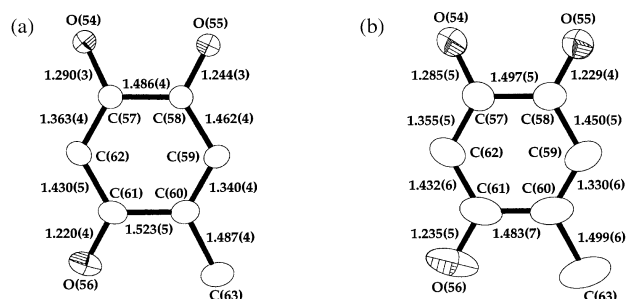


Fig. 4 Views of the $[\text{L}^1]^-$ ligands in the structures of (a) $1 \cdot 0.8\text{CH}_2\text{Cl}_2$ and (b) **2**. The C–C and C–O distances are given to emphasise the predominant 1,4-benzoquinonate resonance form. Details as for Fig. 2.

tronic structure of a 1,4-benzoquinone as shown in Scheme 1, rather than the alternative 4-hydroxy-5-methyl-1,2-benzoquinonate resonance form (Fig. 4). Comparing the two structures, the C(58)–O(55) bond appears to be longer in **1** than in **2**, although the difference between the structures is of borderline significance at exactly 3σ . Such a lengthening would be expected to result from the stronger co-ordination of O(55) to the metal ion in **1** compared to that in **2**. Interestingly, the C(60)–C(61) bond is also significantly lengthened in **1** than in **2**; the reason for this is unclear. All other bond lengths and angles within the $[\text{L}^1]^-$ and $[\text{Tp}^{\text{Ph}_2}]^-$ ligands in the two structures are crystallographically indistinguishable.

Electrochemistry

We were unable to obtain a cyclic voltammogram of $\text{Na}[\text{L}^1] \cdot \text{H}_2\text{O}$ in CH_2Cl_2 –0.5 M NBu_4BF_4 or MeCN –0.1 M NBu_4BF_4 , because of its insolubility in these electrolyte-containing media. However, in dmf –0.1 M NBu_4BF_4 a single reduction process was observed within the solvent window. At 293 K this reduction peak has a complex shape that suggests adsorption of the reduction product at the platinum working electrode surface. However, at 243 K the reduction becomes more classically quasi-reversible, with $E_i = -1.51$ V vs. the ferrocene–ferrocenium couple, and $\Delta E_p = 140$ mV at scan rate (v) = 100 mV s^{-1} . No non-aqueous voltammetry of HL^1 or of any other 2-hydroxybenzoquinone has yet been described. However, in strong aqueous base ($\text{pH} \geq 13$), two groups have reported a reversible 2-electron $[\text{L}^1]^-$ – $[\text{L}^3]^{3-}$ couple close to -0.6 V vs. SCE (ca. -1.0 V vs. Fc/Fc^+).^{9,30} The more negative reduction

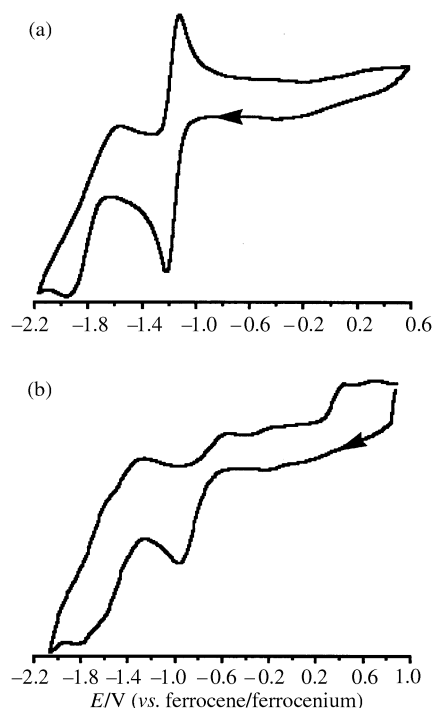


Fig. 5 Cyclic voltammograms in CH_2Cl_2 -0.5 M NBu_4BF_4 at 293 K and $\nu = 100 \text{ mV s}^{-1}$ of (a) complex **2** at 293 K and (b) **1** at 243 K.

potential shown by $\text{Na}[\text{L}^1]\cdot\text{H}_2\text{O}$ in dmf may reflect the lack of hydrogen-bonding solvation interactions, which presumably stabilise the negative charges on the $[\text{L}^1]^-$ and $[\text{L}^3]^{3-}$ anions in aqueous solution.

Cyclic voltammograms of complexes **1** and **2** were obtained in CH_2Cl_2 -0.5 M NBu_4BF_4 at 293 K. The two complexes exhibit rather different electrochemical behaviour. For this reason they will be discussed in order of complexity, with the most simple (**2**) being treated first. In addition to the $[\text{L}^1]^-$ and metal-centered processes discussed in the following paragraphs, **1** and **2** also exhibit an irreversible oxidation in the range $+1.2 \leq E_{\text{pa}} \leq +1.4 \text{ V}$, attributable to oxidation of the $[\text{Tp}^{\text{Ph}_2}]^-$ ligand.²⁴

The cyclic voltammogram of complex **2** contains reductive waves at $E_1 = -1.17$ ($\Delta E_p = 85 \text{ mV}$ at $\nu = 100 \text{ mV s}^{-1}$) and -1.75 V ($\Delta E_p = 380 \text{ mV}$), which are both chemically reversible at $\nu \geq 10 \text{ mV s}^{-1}$ (Fig. 5a). The first of these processes is electrochemically reversible in the range $10 \leq \nu \leq 1000 \text{ mV s}^{-1}$, in that a plot of I_p vs. $\nu^{1/2}$ gave a straight line within this range. However, the more cathodic reduction is not electrochemically reversible, showing a large peak-to-peak separation that increases with increasing ν . A Coulometric determination of the first reduction at 243 K gave $n = 1.1$, consistent with a 1-electron process; determination of the second reduction was impossible because of its proximity to the solvent front. However, since both reductions exhibit similar peak heights (Fig. 5a), the second reduction is almost certainly also a 1-electron reaction. We therefore assign the process at $E_1 = -1.17 \text{ V}$ to a $[\text{L}^1]^-$ - $[\text{L}^2]^{2-}$ couple, and that at -1.75 V to a $[\text{L}^2]^{2-}$ - $[\text{L}^3]^{3-}$ couple. That both of the waves originate from the hydroxyquinonate ligand was confirmed by examining the CV of $[\text{ZnCl}(\text{Tp}^{\text{Ph}_2})]$,³¹ which exhibits no reductive processes within the solvent window under these conditions.

The CV of complex **1** also exhibits two reduction waves. However, in contrast to **2** the first reduction is now quasi-reversible, occurring at $E_1 = -0.71 \text{ V}$ with $\Delta E_p = 360 \text{ mV}$ and $I_{\text{pa}}:I_{\text{pc}} = 0.2:1$ at $\nu = 100 \text{ mV s}^{-1}$. Two irreversible daughter products are associated with this reaction: a major one at $E_{\text{pa}} = +0.49 \text{ V}$, which has approximately half the peak current compared to the parent reduction, and a much weaker wave at $E_{\text{pa}} = +0.73 \text{ V}$. The second reduction is very broad and quasi-

reversible, occurring at $E_2 = -1.6 \text{ V}$. Cooling the solution of **1** to 243 K only slightly improves the chemical reversibility of the first reduction; however, the second reduction becomes resolved into two distinct quasi-reversible processes, at $E_2 = -1.48$ and -1.69 V (Fig. 5b). A Coulometric determination of the first reduction at 293 K yielded $n = 0.95$, consistent with a 1-electron process; again, determination of the second and third waves was not possible. However, since the ratio $I_{\text{pc}}\{\text{first reduction}\}:I_{\text{pc}}\{\text{second and third reductions}\} \approx 1.8:1$, it is likely that the second and third reductions together comprise a 2-electron transformation.

In principle, the first reduction exhibited by complex **1** might be assigned to a $[\text{L}^1]^-$ - $[\text{L}^2]^{2-}$ couple, or a Cu^{II} - Cu^{I} process. We prefer the latter interpretation, on the following grounds. First, the near irreversibility of the first reduction of **1** is in sharp contrast to the reversible $[\text{L}^1]^-$ - $[\text{L}^2]^{2-}$ wave exhibited by **2**. However, other $[\text{Cu}^{\text{II}}(\text{Tp}^{\text{R}})\text{L}_2]^{+}$ complexes exhibit irreversible Cu^{II} - Cu^{I} reductions, with $-0.5 \leq E_{\text{pc}} \leq -1.2 \text{ V}$.^{18,24} Second, the irreversible Cu^{I} - Cu^{II} oxidation of $[\{\text{Cu}(\text{Tp}^{\text{Ph}_2})_2\}_2]$ has been reported to occur at $E_{\text{pa}} = +0.51 \text{ V}$ in CH_2Cl_2 ;²⁶ the first reduction of **1** exhibits a daughter peak at $+0.49 \text{ V}$, which might plausibly be assigned to this process. Third, the second reduction potential of **1** (-1.48 V) is also almost identical to the reduction potential of $\text{Na}[\text{L}^1]\cdot\text{H}_2\text{O}$ in dmf (-1.51 V), suggesting that some decoordination of $[\text{L}^1]^-$ occurs following the initial reduction of **1**. These data all strongly suggest that the first reduction of **1** is a Cu^{II} - Cu^{I} process, and that the expected concomitant structural rearrangement involves substantial decoordination of $[\text{L}^1]^-$ from the Cu^{I} .

Concluding remarks

The reduction potentials exhibited by complex **2** deserve comment, since they differ substantially from those reported for $\text{Na}[\text{Ru}(\text{L}^3)(\text{bipy})_2]\cdot 2\text{EtOH}$, which exhibits $E_1\{[\text{L}^1]^-$ - $[\text{L}^2]^{2-}\} = -0.07 \text{ V}$ and $E_2\{[\text{L}^2]^{2-}$ - $[\text{L}^3]^{3-}\} = -0.97 \text{ V}$ under the same conditions of solvent and temperature used in our work.¹⁶ The much more positive reduction potentials of the ruthenium(II) complex cannot reflect improved $\text{Ru} \rightarrow \text{L}$ ($\text{L} = [\text{L}^1]^-$ to $[\text{L}^3]^{3-}$) π -back bonding, since this would be expected to have the opposite trend of making the ligand more electron rich and so harder to reduce. In addition, $\text{L} \rightarrow \text{Ru}$ π donation cannot be invoked, since this is impossible to a low-spin d^6 metal ion. The more positive reduction potentials shown by $\text{Na}[\text{Ru}(\text{L}^3)(\text{bipy})_2]\cdot 2\text{EtOH}$ compared to those of **2** may reflect the relative degrees of $\text{M}-\text{O}$ ($\text{M} = \text{Ru}$ or Zn) σ covalency in the complexes, since this should be greater for a second row ruthenium(II) transition ion, compared to a first-row zinc(II) ion. In addition, the relative Lewis acidities of Zn^{II} and Ru^{II} could be a factor, since the latter is expected to be more acidic on the basis of the pK_a s of their $[\text{M}(\text{OH}_2)_6]^{2+}$ ions ($\text{M} = \text{Zn}$, $\text{pK}_a = 9.0$;³² $\text{M} = \text{Ru}$, pK_a estimated between 6 and 8³³).

This work has confirmed that $[\text{L}^1]^-$ can be a good ligand to transition metals, binding through the C2 and, if necessary, C1 O atoms (Scheme 1). The $[\text{L}^1]^-$ binding mode in complex **2** is similar to that found in crystal structures of 'TPQ-on' CAO. Combining our results with those of Kaim and co-workers,¹⁶ it can be concluded that coordinated $[\text{L}^1]^-$ undergoes two stepwise 1-electron reductions, whose potentials are very dependent on the nature of the bound metal ion but are consistently separated by 0.8–0.9 V. This contrasts with free $[\text{L}^1]^-$, which undergoes a concerted 2-electron reduction in aprotic media. This has implications for the oxidative half-reaction of CAO, in that there is presently some disagreement whether this occurs by a stepwise¹² or concerted¹³ process. Our results suggest that the former mechanism might only be possible if the reduced co-factor is coordinated to the active-site copper ion during this part of the catalytic cycle.

Experimental

Unless otherwise stated, all manipulations were carried out in air using commercial grade solvents. 1,2,4-trisacetoxy-5-methylbenzene,³⁴ $\text{K}[\text{Tp}^{\text{Ph}_2}]^{27g}$ and $[\text{ZnCl}(\text{Tp}^{\text{Ph}_2})]^{31}$ were prepared by the literature procedures.

Syntheses

$\text{Na}[\text{L}^1]\cdot\text{H}_2\text{O}$. The quinone HL^1 was prepared from 1,2,4-trisacetoxy-5-methylbenzene according to the literature procedure.²⁰ To a solution of this crude solid (4.8 g, 0.035 mol) in MeCN (100 cm³) was added a MeOH (150 cm³) solution of NaOH (1.4 g, 0.035 mol). The mixture was stirred for 30 min, then evaporated to dryness. The resultant dark red solid was washed consecutively with cold MeOH and Et₂O, and dried *in vacuo*. Yield 4.6 g, 83% (Found: C, 46.9; H, 3.7. Calc. for $\text{C}_7\text{H}_5\text{NaO}_3\cdot\text{H}_2\text{O}$: C, 47.2; H, 4.0%). FAB mass spectrum: m/z 177, $[\text{Na}(\text{L}^1)(\text{H}_2\text{O}) - \text{H}]^+$; and 161, $[\text{Na}(\text{HL}^1)]^+$. UV/vis (MeCN): $\lambda_{\text{max}} = 216$ ($\epsilon_{\text{max}} = 2400$), 263 (sh) and 515 nm (140 M⁻¹ cm⁻¹). IR spectrum (Nujol): 1672s, 1638s, 1562w, 1557m, 1293m, 1259s, 1184m, 1131m, 1024w, 1005w, 869s, 832s, 765m, 744m and 732m cm⁻¹. NMR spectra ((CD₃)₂SO, 298 K): ¹H, δ 6.12 (s, 1H, H³), 5.00 (s, 1H, H⁶) and 1.85 (s, 3H, CH₃); ¹³C, δ 190.2 (C¹), 183.4 (C⁴), 171.7 (C²), 151.5 (C⁵), 128.1 (C³), 103.3 (C⁶) and 17.1 (CH₃).

$[\text{Cu}(\text{L}^1)(\text{Tp}^{\text{Ph}_2})] \mathbf{1}$. Reaction of $\text{Na}[\text{L}^1]\cdot\text{H}_2\text{O}$ (0.17 g, 1.0×10^{-3} mol) with $\text{K}[\text{Tp}^{\text{Ph}_2}]$ (0.74 g, 1.0×10^{-3} mol) and $\text{CuCl}_2\cdot 2\text{H}_2\text{O}$ (0.18 g, 1.0×10^{-3} mol) in CH_2Cl_2 (50 cm³) at room temperature for 16 h yielded a deep red solution. Following filtration and concentration, a maroon crystalline solid was obtained upon layering this solution with hexanes. Yield 0.43 g, 55% (Found: C, 71.5; H, 5.4; N, 9.6. Calc. for $\text{C}_{52}\text{H}_{39}\text{BCuN}_6\text{O}_3$: C, 71.8; H, 5.6; N, 9.7%). FAB mass spectrum: m/z 733, $[\text{Cu}(\text{H}^{11}\text{B}\{\text{pz}^{\text{Ph}_2}\}_3)]^+$; 513, $[\text{Cu}(\text{H}^{11}\text{B}\{\text{pz}^{\text{Ph}_2}\}_2)]^+$; and 283, $[\text{Cu}(\text{H}^{11}\text{Bpz}^{\text{Ph}_2})]^+$. UV/vis spectrum (CH_2Cl_2): $\lambda_{\text{max}}/\text{nm}$ ($\epsilon_{\text{max}}/\text{M}^{-1}\text{cm}^{-1}$) 241 (80 400), 315 (sh) and 526 (1700). IR spectrum: (Nujol) 2620w, 1645w, 1614m, 1599m, 1582m, 1548w, 1363m, 1341m, 1250s, 1169s, 1064m, 770m, 750m and 696s cm⁻¹; (CH_2Cl_2) 1650, 1612, 1599, 1581 and 1548 cm⁻¹.

$[\text{Zn}(\text{L}^1)(\text{Tp}^{\text{Ph}_2})] \mathbf{2}$. A mixture of $\text{Na}[\text{L}^1]\cdot\text{H}_2\text{O}$ (0.17 g, 1.0×10^{-3} mol), $\text{K}[\text{Tp}^{\text{Ph}_2}]$ (0.74 g, 1.0×10^{-3} mol) and $\text{Zn}(\text{BF}_4)_2\cdot 2\text{H}_2\text{O}$ (0.18 g, 1.0×10^{-3} mol) in CH_2Cl_2 (50 cm³) was refluxed for 16 h. The orange-red solution was concentrated to approximately half its original volume, filtered, and reconstituted to ca. 2 cm³. Layering this solution with hexanes yielded rust red plates. Yield 0.68 g, 75% (Found: C, 71.0; H, 4.7; N, 9.7. Calc. for $\text{C}_{52}\text{H}_{39}\text{BN}_6\text{O}_3\text{Zn}$: C, 71.6; H, 4.5; N, 9.6%). FAB mass spectrum: m/z 735, $[\text{Zn}(\text{H}^{11}\text{B}\{\text{pz}^{\text{Ph}_2}\}_3)]^+$; and 285, $[\text{Zn}(\text{H}^{11}\text{Bpz}^{\text{Ph}_2})]^+$. UV/vis spectrum (CH_2Cl_2): $\lambda_{\text{max}}/\text{nm}$ ($\epsilon_{\text{max}}/\text{M}^{-1}\text{cm}^{-1}$) 245 (100 800) and 469 (1460). IR spectrum: (Nujol) 2631w, 1658m, 1628m, 1587s, 1546m, 1494w, 1363m, 1284m, 1244s, 1170s, 1074s, 1057s, 916m, 882m, 841m, 816m, 762s, 715w, 693s and 674m cm⁻¹; (CH_2Cl_2) 1657, 1627, 1584 and 1545 cm⁻¹. NMR spectra (CD_2Cl_2 , 298 K): ¹H, δ 7.80–6.92 (m, 30H, Tp^{Ph_2} pz H⁴), 6.56 (s, 3H, Tp^{Ph_2} pz H⁴), 5.71 (s, 1H, L¹ H³), 5.33 (s, 1H, L¹ H⁶) and 1.83 (s, 3H, L¹ CH₃); ¹³C, δ 188.2, 188.0 (L¹ C¹ + C⁴), 163.6 (L¹ C²), 153.7, 151.4 (Tp^{Ph_2} pz C³ + pz C⁵), 150.4 (L¹ C⁵), 132.1, 131.1, 129.8, 128.9, 128.7, 128.5, 128.4, 127.9, 127.8, 127.0, 125.6 (Tp^{Ph_2} Ph C¹⁻⁶ + L¹ C³), 106.5 (L¹ C⁶), 105.2 (Tp^{Ph_2} pz C⁴) and 16.0 (L¹ CH₃).

Single crystal structure determinations

Crystals of formula $[\text{Cu}(\text{L}^1)(\text{Tp}^{\text{Ph}_2})]\cdot 0.8\text{CH}_2\text{Cl}_2$ **1**·0.8CH₂Cl₂ and $[\text{Zn}(\text{L}^1)(\text{Tp}^{\text{Ph}_2})] \mathbf{2}$ were grown by storage of solutions of the complexes in 1:10 CH₂Cl₂–hexanes at –30 °C. Experimental details from the structure determinations are given in Table 2. Both structures were solved by standard heavy atom methods

Table 2 Experimental details for the single crystal structure determinations

	$[\text{Cu}(\text{L}^1)(\text{Tp}^{\text{Ph}_2})]\cdot 0.8\text{CH}_2\text{Cl}_2$ 1 ·0.8CH ₂ Cl ₂	$[\text{Zn}(\text{L}^1)(\text{Tp}^{\text{Ph}_2})]$ 2
Formula	$\text{C}_{52.8}\text{H}_{40.6}\text{B}_2\text{Cl}_{1.6}\text{CuN}_6\text{O}_3$	$\text{C}_{52}\text{H}_{39}\text{BN}_6\text{O}_3\text{Zn}$
M_r	938.22	872.07
Crystal class	Monoclinic	Monoclinic
Space group	$P2_1/c$	$P2_1/c$
$a/\text{\AA}$	16.4602(4)	17.1926(9)
$b/\text{\AA}$	15.9627(4)	10.0741(5)
$c/\text{\AA}$	19.6781(4)	26.6057(11)
$\beta/^\circ$	114.2020(14)	105.775(3)
$U/\text{\AA}^3$	4715.96(19)	4434.5(4)
Z	4	4
$\mu(\text{Mo-K}\alpha)/\text{mm}^{-1}$	0.604	0.605
T/K	150(2)	293(2)
Measured reflections	51153	26956
Independent reflections	10761	8001
R_{int}	0.061	0.064
$R(F)$	0.065	0.052
$wR(F^2)$	0.195	0.164

(SHELXS 97³⁵) and refined by full matrix least squares on F^2 (SHELXL 97³⁶).

$[\text{Cu}(\text{L}^1)(\text{Tp}^{\text{Ph}_2})]\cdot 0.8\text{CH}_2\text{Cl}_2$. The structure contains a badly disordered region of electron density remote from the complex molecule, which was modelled using 5 different orientations of CH₂Cl₂ in a 0.2:0.2:0.2:0.1:0.1 occupancy ratio, giving 0.8CH₂Cl₂ molecules in total. All C–Cl bonds were restrained to 1.83(2) Å, and Cl···Cl 1,3 distances to 2.99(2) Å. The final Fourier difference map contained two residual peaks in the range 1.0–1.2 e Å⁻³, both within this disordered region. All wholly occupied non-H atoms were refined anisotropically, and all H atoms placed in calculated positions.

$[\text{Zn}(\text{L}^1)(\text{Tp}^{\text{Ph}_2})] \mathbf{2}$. No disorder was detected during refinement of this structure. All non-H atoms were refined anisotropically, and no restraints were applied.

CCDC reference number 186/2255.

See <http://www.rsc.org/suppdata/dt/b0/b006700h/> for crystallographic files in .cif format.

Other measurements

Infrared spectra were obtained as Nujol mulls pressed between KBr windows, or in NaCl solution cells, between 400 and 4000 cm⁻¹ using a Nicolet Avatar 360 spectrophotometer, UV/visible spectra with a Perkin-Elmer Lambda 900 spectrophotometer operating between 200 and 1100 nm, in 1 cm quartz cells. All NMR spectra were run on a Bruker ARX250 spectrometer, operating at 250.1 (¹H) and 62.9 MHz (¹³C). Positive ion fast atom bombardment mass spectra were recorded on a VG AutoSpec spectrometer, employing a 3-nitrobenzyl alcohol matrix. CHN microanalyses were performed by the University of Leeds School of Chemistry microanalytical service. X-Band EPR spectra were obtained using a Bruker ER200 spectrometer.

All electrochemical measurements were carried out using an Autolab PGSTAT30 voltammetric analyser, in CH₂Cl₂ or dmf, respectively containing 0.5 or 0.1 M NBu₄BF₄ as supporting electrolyte. Cyclic voltammetric experiments involved the use of platinum disk working and platinum wire counter electrodes, and a Ag–AgCl reference electrode; all potentials quoted are referenced to an internal ferrocene–ferrocenium standard and were obtained at a scan rate of 100 mV s⁻¹, unless otherwise stated. Coulometric determinations were performed in a conventional H-type cell, with a platinum basket working electrode, platinum wire counter electrode and Ag–AgCl reference electrode.

Acknowledgements

The authors gratefully acknowledge funding by The Royal Society (M. A. H.), the EPSRC (C. L. F., X. L.) and the University of Leeds.

References

- 1 J. P. Klinman and D. Mu, *Annu. Rev. Biochem.*, 1994, **63**, 299; J. P. Klinman, *Chem. Rev.*, 1996, **96**, 2541; C. Anthony, *Biochem. J.*, 1996, **320**, 697.
- 2 R. A. Scott and D. M. Dooley, *J. Am. Chem. Soc.*, 1985, **107**, 4348; P. F. Knowles, R. W. Strange, N. J. Blackburn and S. S. Hasnain, *J. Am. Chem. Soc.*, 1989, **111**, 102.
- 3 G. J. Baker, P. F. Knowles, K. B. Pandeya and J. B. Rayner, *Biochem. J.*, 1986, **237**, 609; J. McCracken, J. Peisach and D. M. Dooley, *J. Am. Chem. Soc.*, 1987, **109**, 4064.
- 4 T. J. Williams and M. C. Falk, *J. Biol. Chem.*, 1986, **261**, 15949; D. M. Dooley, M. A. McGuirl, C. E. Cote, P. F. Knowles, I. Singh, M. Spiller, R. D. Brown III and S. H. Koenig, *J. Am. Chem. Soc.*, 1991, **113**, 754.
- 5 D. Mu, K. F. Medzihradsky, G. W. Adams, P. Mayer, W. M. Hines, A. L. Burlingame, A. J. Smith, D. Cai and J. P. Klinman, *J. Biol. Chem.*, 1994, **269**, 9926.
- 6 M. R. Parsons, M. A. Convery, C. M. Wilmot, K. D. S. Yadav, V. Blakeley, A. S. Corner, S. E. V. Phillips, M. J. McPherson and P. F. Knowles, *Structure*, 1995, **3**, 1171; V. Kumar, D. M. Dooley, H. C. Freeman, J. M. Guss, I. Harvey, M. A. McGuirl, M. J. C. Wilce and V. M. Zubak, *Structure*, 1996, **4**, 943; M. C. J. Wilce, D. M. Dooley, H. C. Freeman, J. M. Guss, H. Matsunami, W. S. McIntire, C. E. Ruggiero, K. Tanizawa and H. Yamaguchi, *Biochemistry*, 1997, **36**, 16116; R. Li, J. P. Klinman and F. S. Mathews, *Structure*, 1998, **6**, 293.
- 7 S. M. Janes, D. Mu, D. Wemmer, A. J. Smith, S. Kaur, D. Maltby, A. L. Burlingame and J. P. Klinman, *Science*, 1990, **248**, 981.
- 8 D. M. Dooley, *J. Biol. Inorg. Chem.*, 1999, **4**, 1.
- 9 M. Murae and J. P. Klinman, *J. Am. Chem. Soc.*, 1993, **115**, 7117.
- 10 F. Wang, J.-Y. Bae, A. R. Jacobson, Y. Lee and L. M. Sayre, *J. Org. Chem.*, 1994, **59**, 2409; Y. Lee and L. M. Sayre, *J. Am. Chem. Soc.*, 1995, **117**, 3096; M. Murae and J. P. Klinman, *J. Am. Chem. Soc.*, 1995, **117**, 8707; Y. Lee and L. M. Sayre, *J. Am. Chem. Soc.*, 1995, **117**, 11823.
- 11 M. Murae and J. P. Klinman, *J. Am. Chem. Soc.*, 1995, **117**, 8698.
- 12 D. M. Dooley, W. S. McIntire, M. A. McGuirl, C. E. Cote and J. L. Bates, *J. Am. Chem. Soc.*, 1990, **112**, 2782; D. M. Dooley, M. A. McGuirl, D. E. Brown, P. N. Turowski, W. S. McIntire and P. F. Knowles, *Nature (London)*, 1991, **349**, 262; P. N. Turowski, M. A. McGuirl and D. M. Dooley, *J. Biol. Chem.*, 1993, **268**, 17680; D. M. Dooley and D. E. Brown, *J. Biol. Inorg. Chem.*, 1996, **1**, 205.
- 13 Q. Su and J. P. Klinman, *Biochemistry*, 1998, **37**, 12513.
- 14 N. Nakamura, T. Kohzuma, H. Kuma and S. Suzuki, *J. Am. Chem. Soc.*, 1992, **114**, 6550; S. Suzuki, K. Yamaguchi, N. Nakamura, Y. Tagawa, H. Kuma and T. Kawamoto, *Inorg. Chim. Acta*, 1998, **283**, 260.
- 15 See e.g. R. M. Buchanan, C. Wilson-Blumenberg, C. Trapp, S. K. Larsen, D. L. Green and C. G. Pierpont, *Inorg. Chem.*, 1986, **25**, 3070; G. Speier, S. Tisza, Z. Tyeklar, C. W. Lange and C. G. Pierpont, *Inorg. Chem.*, 1994, **33**, 2041; J. Rall and W. Kaim, *J. Chem. Soc., Faraday Trans. 1*, 1994, 2905.
- 16 E. Waldhör, B. Schwederski and W. Kaim, *J. Chem. Soc., Perkin Trans. 2*, 1993, 2109.
- 17 E. H. Charles, L. M. L. Chia, J. Rothery, E. L. Watson, E. J. L. McInnes, R. D. Farley, A. J. Bridgeman, F. E. Mabbs, C. C. Rowlands and M. A. Halcrow, *J. Chem. Soc., Dalton Trans.*, 1999, 2087; P. Li, N. K. Solanki, H. Ehrenberg, N. Feeder, J. E. Davies, J. M. Rawson and M. A. Halcrow, *J. Chem. Soc., Dalton Trans.*, 2000, 1559.
- 18 M. A. Halcrow, L. M. L. Chia, X. Liu, E. J. L. McInnes, L. J. Yellowlees, F. E. Mabbs and J. E. Davies, *Chem. Commun.*, 1998, 2465; M. A. Halcrow, L. M. L. Chia, X. Liu, E. J. L. McInnes, L. J. Yellowlees, F. E. Mabbs, I. J. Scowen, M. McPartlin and J. E. Davies, *J. Chem. Soc., Dalton Trans.*, 1999, 1753.
- 19 S. Trofimenko, *Scorpionates: The Coordination Chemistry of Polypyrazolylborate Ligands*, Imperial College Press, London, 1999, ch. 1, pp. 18–23.
- 20 L. F. Fieser and M. I. Ardao, *J. Am. Chem. Soc.*, 1956, **78**, 774.
- 21 P. Moënné-Loccoz, N. Nakamura, V. Steinebach, J. A. Duine, M. Mure, J. P. Klinman and J. Sanders-Loehr, *Biochemistry*, 1995, **34**, 7020; N. Nakamura, P. Moënné-Loccoz, K. Tanizawa, M. Mure, S. Suzuki, J. P. Klinman and J. Sanders-Loehr, *Biochemistry*, 1997, **36**, 11479.
- 22 G. J. Gleicher, *The Chemistry of the Quinoid Compounds*, ed. S. Patai, Wiley, New York, 1974, ch. 1, pp. 1–35.
- 23 J. F. Corbett, *J. Chem. Soc. C*, 1970, 2101.
- 24 M. A. Halcrow, E. J. L. McInnes, F. E. Mabbs, I. J. Scowen, M. McPartlin, H. R. Powell and J. E. Davies, *J. Chem. Soc., Dalton Trans.*, 1997, 4025.
- 25 L. M. L. Chia, A. E. H. Wheatley, N. Feeder, J. E. Davies and M. A. Halcrow, *Polyhedron*, 2000, **19**, 109.
- 26 S. M. Carrier, C. E. Ruggiero, R. P. Houser and W. B. Tolman, *Inorg. Chem.*, 1993, **32**, 4889.
- 27 (a) S. G. N. Roundhill, D. M. Roundhill, D. R. Bloomquist, C. Landee, R. D. Willett, D. M. Dooley and H. B. Gray, *Inorg. Chem.*, 1979, **18**, 831; (b) N. Kitajima, K. Fujisawa and Y. Moro-oka, *J. Am. Chem. Soc.*, 1990, **112**, 3210; (c) N. Kitajima, K. Fujisawa and Y. Moro-oka, *Inorg. Chem.*, 1990, **29**, 357; (d) N. Kitajima, K. Fujisawa, T. Koda, S. Hikichi and Y. Moro-oka, *J. Chem. Soc., Chem. Commun.*, 1990, 1357; (e) N. Kitajima, T. Koda, S. Hashimoto, T. Kitagawa and Y. Moro-oka, *J. Am. Chem. Soc.*, 1991, **113**, 5664; (f) J. Perkinson, S. Brodie, K. Yoon, K. Mosny, P. J. Carroll, T. V. Morgan and S. J. Nietzer Burgmayer, *Inorg. Chem.*, 1991, **30**, 719; (g) N. Kitajima, K. Fujisawa, C. Fujimoto, Y. Moro-oka, S. Hashimoto, T. Kitagawa, K. Toriumi, K. Tatsumi and A. Nakamura, *J. Am. Chem. Soc.*, 1992, **114**, 1277; (h) M. Ruff, B. C. Noll, M. D. Groner, G. T. Yee and C. G. Pierpont, *Inorg. Chem.*, 1997, **36**, 4860; (i) S. Itoh, S. Takayama, R. Arakawa, A. Furuta, M. Komatsu, A. Ishida, S. Takamuku and S. Fukuzumi, *Inorg. Chem.*, 1997, **36**, 1407; (j) M. A. Halcrow, J. E. Davies and P. R. Raithby, *Polyhedron*, 1997, **16**, 1535; (k) L. M. L. Chia, S. Radojevic, I. J. Scowen, M. McPartlin and M. A. Halcrow, *J. Chem. Soc., Dalton Trans.*, 2000, 133.
- 28 A. W. Addison, T. N. Rao, J. Reedijk, J. van Rijn and G. C. Verschoor, *J. Chem. Soc., Dalton Trans.*, 1984, 1349.
- 29 N. Kitajima, S. Hikichi, M. Tanaka and Y. Moro-oka, *J. Am. Chem. Soc.*, 1993, **115**, 5496; U. Hartmann and H. Vahrenkamp, *Chem. Ber.*, 1994, **127**, 2381; M. Ruf, R. Burth, K. Weis and H. Vahrenkamp, *Chem. Ber.*, 1996, **129**, 1251; M. Ruf, K. Weis, I. Brasack and H. Vahrenkamp, *Inorg. Chim. Acta*, 1996, **250**, 271; M. Ruf, K. Weis and H. Vahrenkamp, *Inorg. Chem.*, 1997, **36**, 2130; K. Weis, M. Rombach, M. Ruf and H. Vahrenkamp, *Eur. J. Inorg. Chem.*, 1998, 263; K. Weis and H. Vahrenkamp, *Eur. J. Inorg. Chem.*, 1998, 271.
- 30 W. Flaig, H. Beutelspacher, H. Reimer and E. Kälke, *Liebigs Ann. Chem.*, 1968, **719**, 96.
- 31 R. Alsasser, A. K. Powell, S. Trofimenko and H. Vahrenkamp, *Chem. Ber.*, 1993, **126**, 685.
- 32 D. W. Barnum, *Inorg. Chem.*, 1983, **22**, 2297.
- 33 M. Stebler-Röthlisberger, W. Hummel, P.-A. Pittet, H.-B. Bürgi, A. Ludi and A. E. Merbach, *Inorg. Chem.*, 1988, **27**, 1358.
- 34 J. Thiele and E. Winter, *Liebigs Ann. Chem.*, 1900, **31**, 341.
- 35 G. M. Sheldrick, *Acta Crystallogr., Sect. A*, 1990, **46**, 467.
- 36 G. M. Sheldrick, SHELXL 97, Program for the refinement of crystal structures, University of Göttingen, 1997.